RESEARCH ARTICLE OPEN ACCESS

Assessment of the Mechanical and Hydraulic Performance of Kenaf Fiber Geotextiles for the Reinforcement of Road Foundation Layers



ISSN: 1874-1495

Dieudonné Tankoano¹, Hamma Fabien Yonli^{1,*}, Sidpouita Mathilde Koudougou², Médaninpo Fidèle Yonli¹, Wendqoudi Emmanuel Nikièma³ and David Yemboini Kader Toquyeni²

¹Graduate School of Engineering, Yembila Abdoulaye Toguyeni University, BP 46 Fada N'Gourma, Burkina Faso ²Institute of Industrial and Textile Systems Engineering, Polytechnic School of Ouagadougou, 08 BP 143 Ouagadougou 08, Burkina Faso

³Department of Soil and Foundation Engineering Studies, National Laboratory for Building and Public Works, BP 133 Ouagadougou 01, Burkina Faso

Abstract:

Introduction: The use of geotextiles is now well established in the field of civil engineering, particularly in geotechnics, where they serve a range of functions including drainage, filtration, separation, reinforcement, protection, and erosion control. For over three decades, these materials have played a key role in the design and long-term performance of infrastructure. The development of geotextiles made from natural plant fibers, especially those derived from kenaf, represents a promising advancement that offers both economic and environmental benefits. This study aims to evaluate the mechanical and hydraulic properties of woven geotextiles made from kenaf fibers sourced from Nérékourosso, as well as their effectiveness in reinforcing road foundation layers.

Methods: Two types of geotextiles were produced by weaving, with mesh openings of 0 mm and 5 mm, respectively. Mechanical characterization tests were carried out, along with static puncture resistance and normal-to-plane permeability tests. CBR load-bearing tests were performed to evaluate reinforcement efficiency depending on the geotextile's position in the foundation layer. Mechanical tests showed higher tensile strength in the cross direction for the geotextile with no mesh opening (17.19 kN/m) compared to the 5 mm mesh type (2.90 kN/m).

Results: The closed-mesh geotextile withstood a maximum puncture load of 1170 N, versus 540 N for the open-mesh variant. The 0 mm mesh geotextile exhibited a surface flow rate of 2200 L/min/m². CBR tests indicated better performance for the 5 mm mesh geotextile, especially when placed at mid-height within the reinforced layer.

Discussion: These results suggest that while the closed-mesh geotextile offers superior intrinsic mechanical properties due to its dense structure, the open-mesh variant performs better in soil reinforcement applications, likely because its structure allows better interaction with surrounding materials and more effective stress distribution.

Conclusion: Kenaf-based woven geotextiles show promising potential for road foundation reinforcement, with mesh configuration significantly influencing performance.

Keywords: Woven geotextiles, Foundation layer reinforcement, Static puncture, Bearing capacity, Kenaf fibers.

 $\ensuremath{\texttt{©}}$ 2025 The Author(s). Published by Bentham Open.

This is an open access article distributed under the terms of the Creative Commons Attribution 4.0 International Public License (CC-BY 4.0), a copy of which is available at: https://creativecommons.org/licenses/by/4.0/legalcode. This license permits unrestricted use, distribution, and reproduction in any medium, provided the original author and source are credited



Cite as: Tankoano D, Yonli H, Koudougou S, Yonli M, Nikièma W, Toguyeni D. Assessment of the Mechanical and Hydraulic Performance of Kenaf Fiber Geotextiles for the Reinforcement of Road Foundation Layers. Open Civ Eng J, 2025; 19: e18741495424845. http://dx.doi.org/10.2174/0118741495424845251112103116



Received: August 08, 2025 Revised: September 09, 2025 Accepted: September 17, 2025 Published: November 28, 2025



Send Orders for Reprints to reprints@benthamscience.net

1. INTRODUCTION

Infrastructure development is a fundamental driver of a country's economic growth. Roads, buildings, and engineering structures constitute an important foundation for a nation's socio-economic dynamism. However, these infrastructures only fulfill their role as pillars of development if they are constructed to high standards of quality and sustainability [1, 2]. Modern construction faces a major challenge: the poor quality of many sites, exacerbated by the increasing scarcity of soils with favorable geotechnical characteristics—particularly as a result of rapid urbanization and industrialization [3]. This phenomenon leads to structural issues, such as differential settlement and the premature deterioration of infrastructure [4, 5].

Given these geotechnical constraints, the use of reinforcement solutions has become essential. Geotextiles represent an innovative and effective approach. Widely used in road geotechnics, these materials enhance the mechanical performance of soils by providing improved tensile strength and limiting particle displacement [6, 7]. Geotextiles reinforce road structures and contribute to their durability. However, their production raises environmental concerns. Made from petroleum-derived polymers (polypropylene, polyester, polyethylene), they are non-renewable and have a significant ecological footprint [8]. To address this dual technical and environmental challenge, this study proposes the development of an eco-friendly geotextile for reinforcing foundation layers, using natural kenaf fibers.

Numerous studies have demonstrated the benefits of incorporating fibers into construction materials to improve their mechanical properties. For example, nylon fibers from waste tires have been reported to enhance the dynamic modulus and rutting resistance of asphalt mixtures [9], while recycled textile fibers contribute to increased fatigue resistance through a microcrack "stitching" effect [10]. Treated aramid fibers provide gains in tensile strength, although their effectiveness strongly depends on the quality of dispersion [11]. Finally, biomass fibers, such as bamboo and corn straw, represent a sustainable alternative to synthetic fibers, improving durability and resistance to moisture-induced damage [12].

The solution explored in this study constitutes a high-performance alternative capable of substantially enhancing the soil's geotechnical properties, while preserving its natural structure and environmental integrity [13]. The use of kenaf fibers, derived from a renewable resource available in Burkina Faso, aims to combine mechanical performance with ecological sustainability. Kenaf fiber (*Hibiscus cannabinus* L.) is often considered more suitable than other natural fibers, such as jute and coconut fiber, particularly for applications in construction, composites, and engineering, due to several physico-mechanical and environmental characteristics. Kenaf fiber offers notable advantages over jute, including higher mechanical strength and elastic modulus, combined

with a low density that improves the strength-to-weight ratio. Its reduced lignin content promotes better adhesion to matrices and limits the need for treatments, while its lower sensitivity to moisture ensures better dimensional stability compared to jute [14, 15]. In contrast to coconut fiber, which is too elastic for applications requiring rigidity, kenaf provides an optimal balance between stiffness and durability. Moreover, its rapid growth, high yield, and low agricultural input requirements make it a sustainable resource [16] and a competitive one, particularly suitable for composites, construction materials, and insulation applications, thus extending its range of use beyond that of jute and coconut [17].

Kenaf is a plant that has long been used for its fibers, traditionally employed in mask making or as rope in many parts of Burkina Faso. Studies, such as those by Muthu [18], have shown that natural fibers can offer performance comparable to synthetic fibers in certain applications, particularly for temporary solutions like erosion control and drainage.

Furthermore, according to Millogo et al. [17], kenaf fibers possess good mechanical properties (tensile strength, modulus of elasticity) and can be integrated into geotextiles to reinforce road foundation layers. Kenaf fibers also exhibit strong potential in the textile sector due to their physical and mechanical properties, which are comparable to, or even superior to, those of other fibers from the same family, the bast fibers. This makes them suitable for a wide range of textile applications, whether for conventional or technical uses [18].

Thus, the overall objective of this work is to improve the bearing capacity of weak subgrades to enable the construction of reliable infrastructure while minimizing environmental impact.

2. MATERIALS AND METHODS

2.1. Study Design

This study employs an analytical and experimental approach to evaluate the mechanical and hydraulic performance of kenaf fiber geotextiles used to reinforce road foundation layers. The experimental design comprised three main phases: (i) fabrication and characterization of kenaf-based geotextiles with different meshing openings, (ii) laboratory testing of mechanical and hydraulic behavior, and (iii) comparative performance assessment in soil reinforcement scenarios.

The study uses a quantitative approach focused on laboratory testing. The measured variables include, on one hand, the thickness, surface mass, hydraulic conductivity, and tensile strength of the geotextiles, and on the other hand, the bearing capacity of reinforced soils, assessed through the CBR index.

2.1.1. Literature Review Strategy

A literature review was conducted to guide the choice of test parameters and to discuss the results. It focused on studies generally published between 2014 and 2024, searching the ScienceDirect, SpringerLink, Scopus, and

Google Scholar databases. The keywords used included "kenaf fiber geotextile," "natural fiber reinforcement," and "CBR test with geotextiles." Studies that did not present experimental data or that used only synthetic geotextiles were excluded. The selection process extracted relevant data for a comparative synthesis.

2.1.2. Sample Size and Experimental Units

In this study, the experimental units consisted of samples of natural geotextiles alone and soil-geotextile configurations subjected to mechanical testing, with or without reinforcement. To determine the physical properties of the geotextiles, ten samples were used. Mechanical tests were performed on both the geotextiles alone and on soils with or without reinforcement with three repetitions for each configuration, and the results were expressed as the average of the measured values. The same approach was adopted for the hydraulic characterization. All tests were performed under strictly identical environmental and compaction conditions to ensure the comparability of results.

2.1.3. Testing Procedures and Data Analysis

Mechanical and hydraulic tests were performed in accordance with ASTM, AFNOR and ISO standards. Based on the data obtained, a comparative analysis was conducted to assess the influence of geotextile type on soil behavior. Graphs were generated using MS Excel software.

2.2. Origin and Physico-chemical Properties of Kenaf Fibers

The kenaf fibers used in this study were collected in the municipalities of Ouri and Tchiériba, both located in the province of Balès, within the Boucle du Mouhoun region of Burkina Faso. Chemically, these fibers have a composition comparable to that of other plant fibers commonly used in industrial applications. They are characterized by a cellulose content of 45%, a hemicellulose content of 18%, a lignin content of 21%, and a pectin content of 14%. Furthermore, measurements indicate that the average diameter of these fibers is

around 105 micrometers, making them suitable for use in geotextiles.

2.3. Manufacture of Geotextiles

The geotextiles were woven from yarns obtained from kenaf fibers by hand spinning (Fig. 1).

The geotextiles were woven according to two models: one without mesh openings (0 mm), identified as GTX 0 mm, and the other with 5 mm openings, identified as GTX 5 mm. These choices were mainly based on technical considerations.

According to the literature, geotextiles with a closed structure have the best mechanical characteristics [19]. Both types were woven manually. They were designed using the plain weave pattern, which is the strongest weave and most resistant to abrasion due to its short undulations between the threads [20]. Figs. (2 and 3) illustrate the weaving process and the products obtained.

The closed-mesh geotextile (0 mm) is commonly used for its high mechanical strength, with the density of its weave providing excellent tensile resistance and good reinforcement capacity. The open-mesh geotextile (5 mm) combines strength and permeability, ensuring both drainage and filtration. However, the choice of mesh size does not depend solely on technical criteria, but also on design and manufacturing constraints. In the case of manual weaving, it is particularly challenging to produce openings smaller than 5 mm, which justifies the choice of a minimum 5 mm opening.

The remainder of this study is devoted to characterizing the geotextiles obtained, with a focus on their mechanical, hydraulic, and physical properties. This step aims to evaluate their performance and determine their suitability for civil engineering applications, particularly in soil reinforcement and stabilization.

2.4. Physical Characterization of Geotextiles

Two key properties of geotextiles were determined: thickness, which influences their ability to separate, filter, and protect; and mass per unit area, an overall indicator of the geotextile's quality, strength, and durability.







Fig. (1). Raw kenaf fibers (a), manual spinning of the fibers (b), and yarns produced from spinning (c).

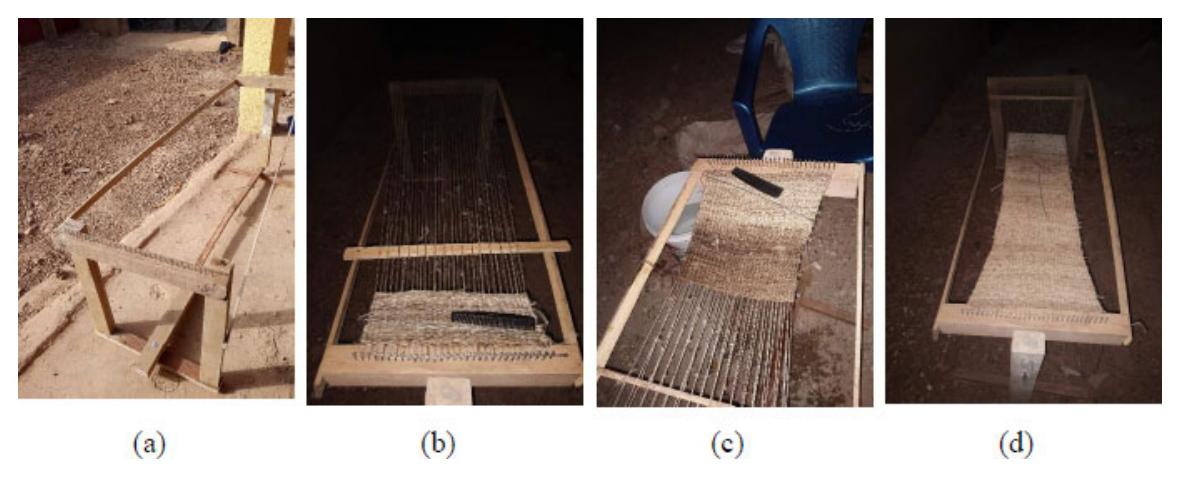


Fig. (2). Weaving machine for 0 mm geotextile (a), weaving process for 0 mm geotextile (b, c), and final woven product (d).

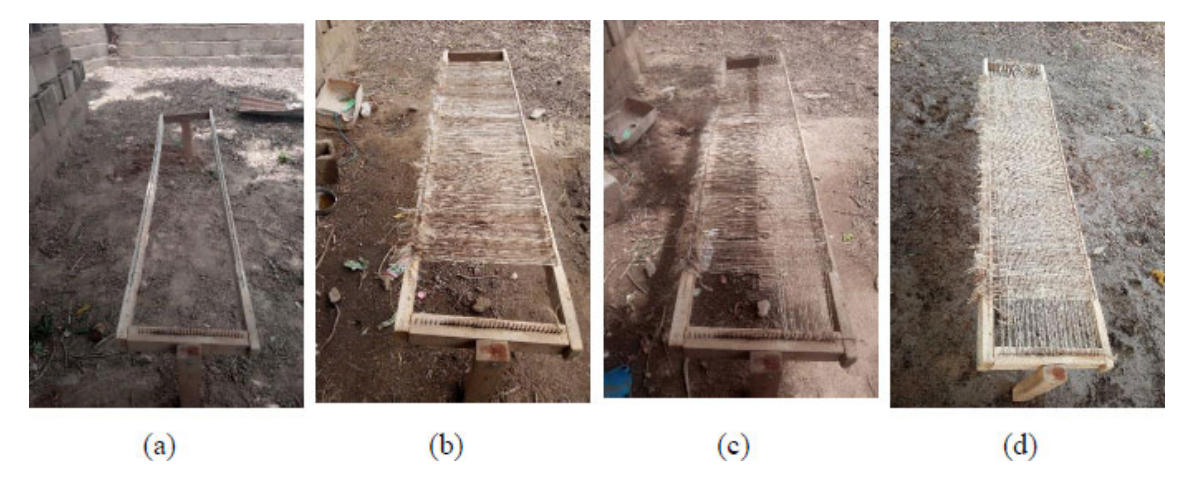


Fig. (3). Weaving machine for 5 mm geotextile (a), weaving process for 5 mm geotextile (b and c), and final woven product (d).

2.4.1. Determination of the Geotextile Thickness

To determine the thickness of the geotextiles, ten samples were taken from each type (0 mm and 5 mm mesh openings), in accordance with the requirements of European standard NF EN ISO 9862. Each sample, cut according to standard NF EN ISO 9863-1, has a surface area of 100 mm \times 100 mm, with a tolerance of \pm 2 mm. The test consisted of applying a specific pressure of 2 kPa (± 0.01) to each sample, placed between two plates, for 30 seconds, in accordance with the standard NF EN ISO 9863-1. A micrometer was used to measure the thickness of the samples. This instrument operates by applying a defined pressure to the sample placed between two plates, then reading the distance between the ends of the micrometer. This distance corresponds to the thickness of the geotextile. The samples were cut using scissors. Fig. (4) illustrates the procedure for measuring the thickness of the geotextiles.

2.4.2. Determination of the Surface Mass of Geotextiles

The determination of the surface mass required the use of ten samples for each type of geotextile (0 mm and 5 mm mesh openings), as was done for the thickness measurement. The number of samples is defined by the standard NF EN ISO 9862. Each sample had the same dimensions as those used to determine thickness, i.e., 100 mm \times 100 mm, in accordance with the above-mentioned standard. The test was governed by standard NF EN ISO 9864 (October 2005). It involves measuring the mass of each sample and then relating this value to its surface area to calculate the surface mass. To do this, the samples were cut using scissors and weighed using a KERN precision scale.

The surface mass σ was determined using the following formula in Eq (1):

$$\sigma\left(g/m^2\right) = \frac{m}{S} \tag{1}$$

where m is the mass of the geotextile sample, and S is its surface area.

Figure 5 illustrates the procedure for measuring the surface mass of the geotextiles.

2.5. Mechanical Characterization

The tensile strength and puncture resistance of geotextiles were evaluated in order to characterize their mechanical behavior under tensile forces and concentrated local stresses commonly encountered in civil engineering applications.

2.5.1. Tensile Test

The tensile test on geotextiles was carried out in both directions (production direction and cross direction) in accordance with European standard EN 10319 (2015).

This standard recommends a minimum of five test samples for each direction.

The test samples were cut in accordance with ISO.

The test samples were cut in accordance with ISO 9862, which specifies a nominal width of 20 mm per sample. A total of twenty test samples were prepared using scissors for the tensile test, distributed as follows:

- Five test samples in the production direction and five (5) in the cross direction for the 0 mm geotextile,
- Five test samples in the production direction and five (5) in the cross direction for the 5 mm geotextile.

The samples were taken from across the entire width of the geotextile in order to represent all parts of it. Once cut, they were fixed one by one to the tensile testing machine, maintaining a distance of 100 mm between the jaws. The tensile testing machine used was a UtilCell 650S/FD 5017 model, serial number 1113680 (12) i.





Fig. (4). Micrometer (a), measuring the thickness of a geotextile test sample (b).







Fig. (5). 0 mm geotextile samples (a) and 5 mm geotextile samples (b) used for surface mass determination, and the precision balance used for weighing (c).

The test consisted of holding the test sample between the jaws of a tensile testing machine (Fig. 6), which applied a constant longitudinal force until the sample broke. The tensile properties were then calculated from the values read on the machine's dial. The main measurements recorded were: the breaking force (maximum load) and the final length of the test sample after traction.

The tensile characteristics were then determined using the following formulas:

$$\Delta l = l - l_0 \tag{2}$$

where Δl is the elongation, l is the final length, and l_0 is the initial length.

$$R = \frac{F}{l_0}$$
 (3)

where R is the tensile strength expressed in kN/m and F is the maximum force.

$$\mathcal{E} = \frac{\Delta l}{l_0} \times 100 \tag{4}$$

Where E is the deformation expressed as a percentage (%).

Figure 6 shows the tensile testing machine used and the test procedure.

2.5.2. Puncture Testing on Geotextiles

The puncture resistance test on a geotextile was performed by placing a test sample on a CBR mold. A riser was then positioned above the geotextile to stabilize it. The assembly (mold, riser, and geotextile) was consolidated and secured with nuts to ensure optimal support. The mold was then placed on a CBR press, which applied a puncture force at a constant speed of 1.28 mm/min until the geotextile broke due to excessive elongation. The CBR press punch was circular in shape with a diameter of 50 mm and a height of 150 mm. A total of five samples were used for this test. Fig.7 illustrates the punching procedure used to determine the geotextile's resistance to puncture.

2.5.3. Punching Test on Soils reinforced with **Geotextiles**

In order to evaluate the reinforcement capacity of the geotextile in soil, four CBR tests were carried out, following AFNOR NF P 94-093 standards. The material studied was sourced from a borrow area identified as part of the National Road 4 (RN4) widening project; it is intended to serve as a foundation layer for the access road leading to Thomas Sankara University, located east of the city of Ouagadougou. Modified Proctor and CBR tests were previously carried out on this soil. The results of the tests on the reference soil are summarized in Table 1.







(c) Fig. (6). Tensile testing machine (a), tensile testing on a GTX 0 mm test sample (b), tensile testing on a GTX 5 mm test sample (c).

Table 1. Proctor characteristics and CBR values of the material at different levels of relative compactness.

Davismatisma	Proctor		CBR		
Designations	$\gamma_{dmax}(g/cm^3)$	ω _{opt} (%)	CBR at 98% OPM	CBR at 95% OPM	CBR at 90% OPM
Values	2.075	10.3	90	58	16

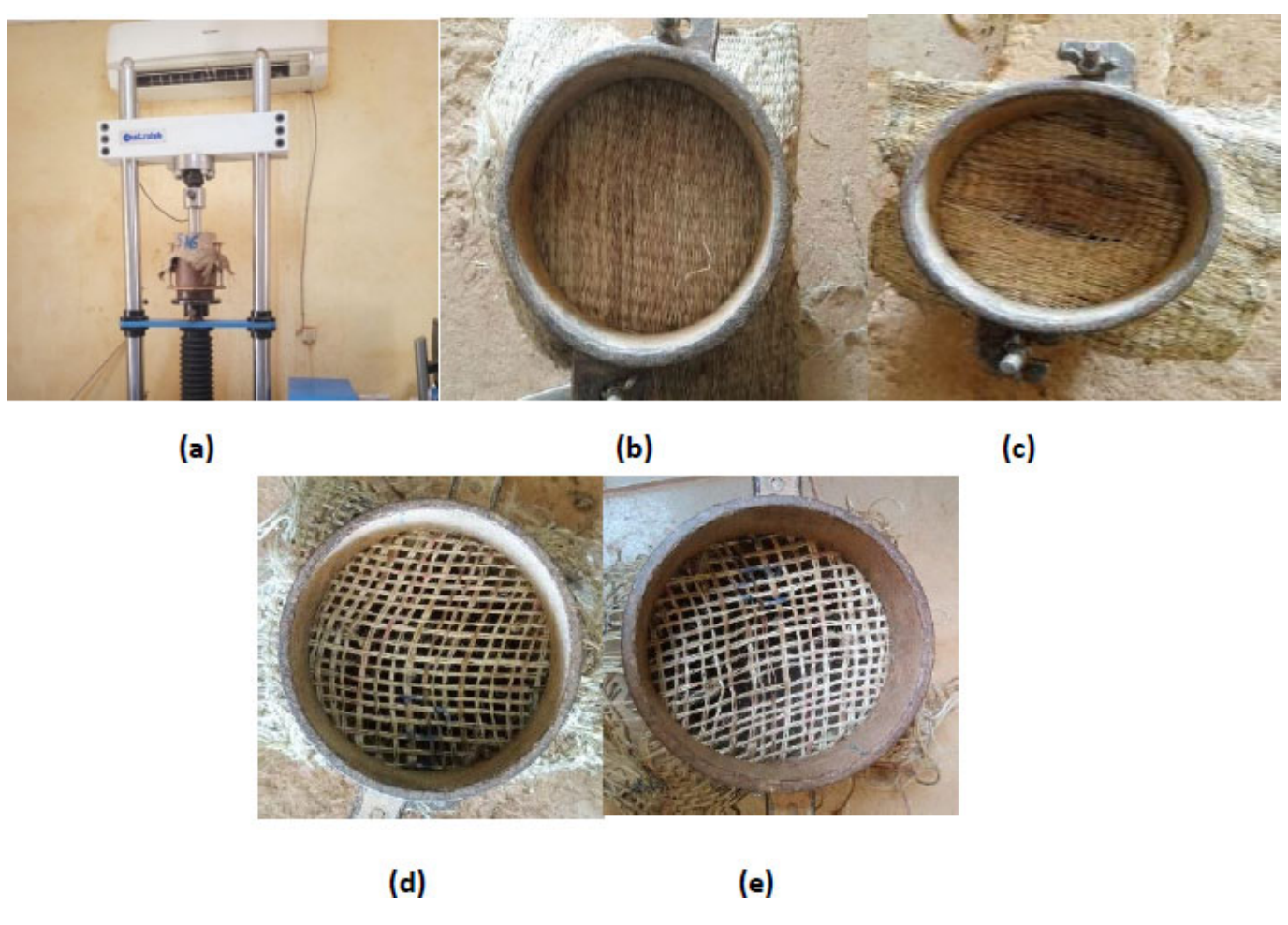


Fig. (7). Assembly (geotextile and mold) mounted on the CBR press (a), 0 mm geotextile before (b) and after punching (d), 5 mm geotextile before (c) and after punching (e).

The first two tests were carried out with a geotextile having $0\ mm$ mesh opening:

- The first test consisted of placing a layer of geotextile halfway up the CBR mold from the base of the mold.
- The second test was carried out by placing two layers of geotextile, respectively at one-third (1/3) and two-thirds (2/3) of the height of the mold.

The same protocol was repeated with a geotextile having a 5 mm mesh opening.

Indeed, in the first scenario, a single layer was placed at mid-height to intercept the zone of maximum shear generated by the plunger, where the geotextile most effectively mobilizes its tensile action and modifies the failure mode [21-23]. In the second scenario with two layers, positioning them at 1/3 and 2/3 of the height allows coverage of the entire plastic zone, ensures a more

uniform reinforcement distribution, and improves both bearing capacity and settlement control, which is consistent with experimental results reporting an optimum near 1/3 of the height [24-26].

The press used for these tests was the same as that used previously for punching the geotextile. The samples were compacted at 56 blows, 25 blows, and 10 blows in accordance with standard NF P94-078.

The samples are rated as follows:

- Soil + GTX 0 (01): reference soil (clayey lateritic gravel) with a 0 mm geotextile layer,
- Soil + GTX 0 (02): reference soil with two 0 mm geotextile layers,
- Soil + GTX 5 (01): reference soil with a 5 mm geotextile layer,
- Soil + GTX 5 (02): reference soil with two 5 mm geotextile layers.

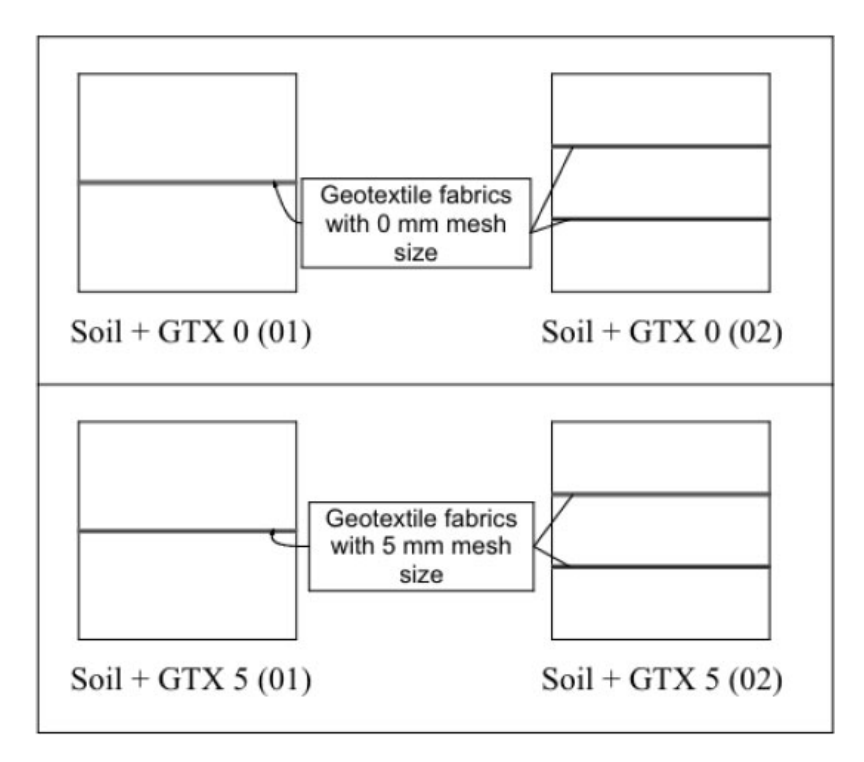


Fig. (8). Position of geotextile layers within the CBR test samples.

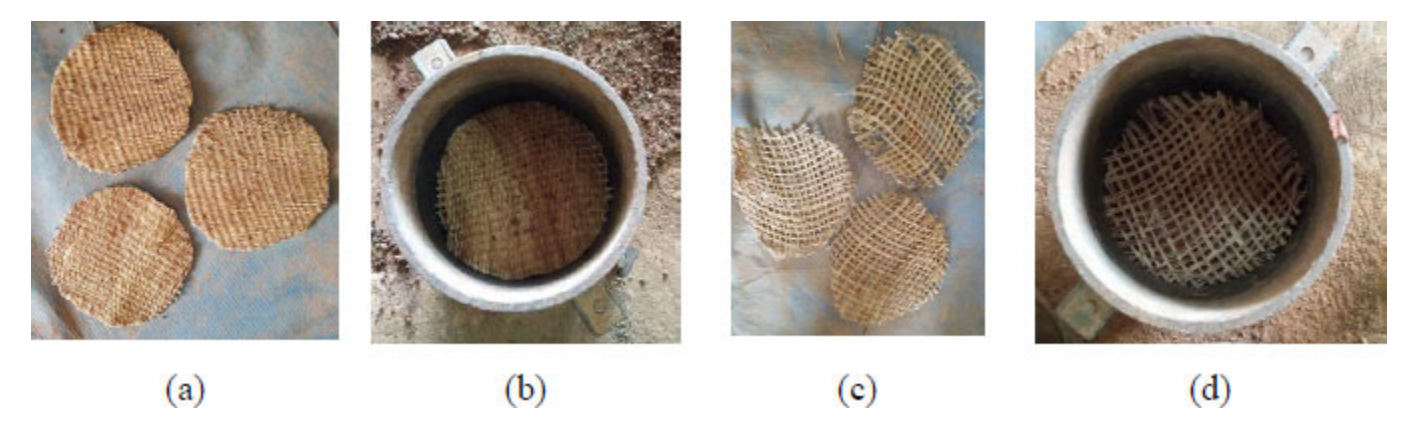


Fig. (9). 0 mm geotextile samples cut (a) and placed halfway up the mold (c); 5 mm geotextile samples cut (b) and placed halfway up the mold (d).

The location of the geotextiles in the samples is illustrated in Figs. $(8 \ \text{and} \ 9)$ shows the samples cut and placed in the mold.

2.6. Hydraulic Characterization

Water permeability is a very important criterion for reinforcement. The normal permeability of a geotextile measures its ability to allow water to pass through it perpendicularly to its plane. In the presence of water, soil loses its cohesion and therefore its strength decreases. Based on this analysis, the 0 mm geotextile can act as an obstacle if it is not sufficiently permeable. This is the

reason why permeability tests were only conducted on the 0 mm geotextile, whose very closed structure could create a clogging effect or act as a hydraulic barrier. For the 5 mm geotextile, the large mesh opening is assumed to provide sufficient permeability, in accordance with criteria established in the literature and standards.

The principle of the normal permeability test is based on the application, without constraint, of a unidirectional flow of water perpendicular to the plane of a layer of geotextile, within a well-defined range of water heights. The test is described in standard ISO 11058 (May 2019). For this test, five test samples with dimensions compatible

with the permeability apparatus are required. Before the measurements, they are immersed in water for 12 hours to ensure they are saturated. The test consists of attaching the geotextile test sample to the lower end of a funnel. A defined quantity of 100 mL of water is then measured and poured into the funnel. At the same time, a stopwatch is activated to measure the time required for the water to drain completely through the geotextile. The flow rate in plane D is calculated using the following formula:

$$D\left(m^{3}/s\right) = \frac{Q}{t} \tag{5}$$

With Q: the volume of water (m^3) poured into the funnel, and t: the time (s) taken by the geotextile to drain the water. From this formula, we can deduce the specific flow rate Ds. Ds is based on the geotextile sample surface area S, expressed in $L/min/m^2$.

$$Ds (L/min/m^2) = \frac{Q}{t \times S}$$
 (6)

The permeability coefficient k is calculated using the following formula:

$$k(m/s) = \frac{D}{s} \tag{7}$$

With s: the surface area of the lower end of the funnel.

3. RESULTS AND DISCUSSION

3.1. Physical characteristics

The results of the physical characterization are summarized in Table 2.

The average thicknesses of geotextiles are 2.27 mm for the 0 mm mesh opening geotextile (GTX 0) and 0.84 mm for the 5 mm mesh opening geotextile (GTX 5). This difference in thickness is likely due to the structure of the mesh. GTX 0 is produced by tightly closing almost all of its meshes using a comb, giving it a more compact structure than the 5 mm geotextile. This increased compactness explains why GTX 0 is nearly three times thicker than GTX 5.

The tests revealed a surface mass of 828 g/m^2 for the 0 mm geotextile and 313 g/m^2 for the 5 mm geotextile, as shown in Table 2. This difference is likely due to the larger mesh openings of the 5 mm geotextile.

It is worth noting that the thickness results (CV < 5%) demonstrate good homogeneity. In contrast, for the surface weight (5% < CV < 15%), the coefficients of variation indicate a moderate variability. Overall, these data nevertheless reflect a satisfactory reproducibility of the measurements.

3.2. Mechanical Characteristics

Table ${\bf 3}$ provides the results of the tensile tests on GTX 0 and GTX 5.

The maximum resistance of kenaf geotextiles with a 0 mm mesh opening (GTX 0) is 2.37 kN/m in the production direction and 17.19 kN/m in the cross direction. For

geotextiles with a 5 mm mesh opening (GTX 5), the values are 2.85 kN/m and 2.90 kN/m, respectively. Overall, the results indicate that kenaf geotextiles exhibit better performance in the cross-direction than in the production direction. These data highlight the impact of mesh openings on the tensile strength of geotextiles. For GTX 5, the strengths are similar in both directions, while for GTX 0, they are very different: the strength in the cross direction is about seven times greater than that in the production direction. This difference could be related to the spacing between the warp threads.

Compared to the 0 mm geotextile, the cross-direction strength of the kenaf geotextile is higher than that of the coconut geotextile. However, its production direction strength is seven times lower, which leads to the conclusion that, in general, coconut geotextile performs better than kenaf geotextile in terms of tensile strength.

However, when comparing these results with those of Texel SX-60T, SX-90T, SX-110T, and SX-130T polypropylene-reinforced woven geotextiles, the kenaf geotextile performs well. In fact, the maximum tensile strength of Texel geotextiles varies between 890 and 1402 N/m [27], while the lowest tensile strength obtained with kenaf geotextiles is 2370 N/m. These excellent tensile properties of kenaf geotextiles are probably due to the good mechanical and chemical characteristics of kenaf fibers [17-29].

Static puncture testing was performed on the geotextiles, and the results of these experiments are shown in Table ${\bf 4}$.

The maximum static puncture resistance values for the geotextiles are 1.17 kN for the 0 mm mesh geotextile (GTX 0) and 0.54 kN for the 5 mm geotextile (GTX 5). Once again, there is a significant difference between these two types of geotextiles. The puncture resistance of GTX 0 is more than twice that of GTX 5, a disproportion that appears to be directly related to the mesh openings. In view of the previous results on tensile strength, the weft threads likely play a major role in this disparity in puncture resistance between GTX 0 and GTX 5. The good performance of the kenaf geotextile can likely be attributed to its weight per unit area. The puncture resistance of geotextiles is influenced by several parameters, including the manufacturing process, weight per unit area and thickness [30].

3.2.1. Comparative Analysis of the Mechanical Performance of Geotextiles

According to the literature and technical data sheets, the higher the surface mass, the better the geotextile has tensile and punching resistance [31]. This study supports this theory because the 0 mm mesh geotextile, with a higher surface mass, also exhibits the best tensile and punching resistance.

The geotextiles examined in our study exhibit significantly lower mechanical performance compared with commercially available industrial products. Consider, for example, a lightweight geotextile: our results indicate

a tensile strength of approximately 2.9 kN/m, whereas typical specifications for a short-fiber product of comparable mass, according to industrial standards, report a minimum value of 11.3 kN/m. Similarly, the CBR puncture resis-tance of our sample (0.54 kN) is well below the standard value of 1.78 kN [32].

For heavier samples (828 g/m²), the performance of our geotextiles (tensile strength in the production direction = 2.37 kN/m; puncture resistance = 1.17 kN) also remains far below that of industrial products. For instance, an 800 g/m² needle-punched geotextile typically exhibits a tensile strength of 25 kN/m, a CBR puncture resistance of 4 kN, and a thickness of approximately 5 mm

[33]. Furthermore, Sikaplan-800, which is used in demanding protection and separation applications, achieves tensile strengths of 55~kN/m (in both production and cross directions) and a static punching resistance of 9.5~kN [34].

These deviations may result from differences in the type and quality of fibers, needling density, manufacturing processes, and possible variations in anisotropy or test execution.

3.4. Hydraulic Characteristics

The hydraulic characteristics are summarized in Table 5.

Table 2. Thicknesses of geotextiles.

Designations	Thickness (mm)	Coefficient of Variation	Surface weight (g/m²)	Coefficient of Variation (CV) of surface weight (%)
Sample	Timekness (min)	(CV) of thickness (%)		
Geotextile with 0 mm mesh opening (GTX 0)	2.27 ± 0.02	0.77	828 ± 57	10.86
Geotextile with 5 mm mesh opening (GTX 5)	0.84 ± 0.05	3.12	313 ± 26	13.35

Table 3. Tensile test results.

Designations	Geotextile with 0 mm me	sh opening (GTX 0)	Geotextile with 5 mm mesh opening (GTX 5)		
Designations	Production direction	Cross direction	Production direction	Cross direction	
Maximum load (kN)	0.27±0.04	1.72±0.41	0.31±0.05	0.314±0.05	
Elongation Δl at failure (cm)	1.24±0.22	2.81±0.59	1.52±0.18	1.53±0.21	
Tensile strength (kN/m)	2.37±0.51	17.19±3.58	2.85 ± 0.27	2.9 ± 0.40	
Deformation E at failure (%)	10.91±1.46	28.5±6.71	14.04±1.71	14.20±2.11	

Table 4. Puncture test results.

Designations	Geotextile 0 mm	Geotextile 5 mm
Maximum load (N)	1170	540
Penetration at failure (mm)	10.07	11.6

Table 5. Hydraulic characteristics of geotextiles.

Designations	Geotextile 0 mm
D (m³/s)	1.52 x 10 ⁵ ± 1.18 x 10 ⁶
K (m/s)	$3.67 \times 10^{-2} \pm 2.79 \times 10^{-3}$
Ds (L/min/m²)	2200.6 ± 168.5

The average values for the flow rate and permeability of the 0 mm kenaf geotextile (GTX 0) are 1.52×10^{-5} m³/s and 3.67×10^{-2} m/s, respectively. When reported in L/min/m², the average flow rate reaches 2200.6 L/min/m². These results indicate that GTX 0 is suitable for filtration, given its high flow rate capability. We deduce that the hydraulic properties of GTX 5 are also adequate. Compared to the Texel SX 104F filtration geotextile, its flow rate is three times higher. This performance is

reassuring for its use in reinforcement, as it allows for good water flow, an essential parameter in this function.

3.5. Analysis of the Behavior of Geotextiles Integrated into Soils

After the tests, the results were obtained by calculating the bearing capacity and plotting the load-penetration curves for the reference soil and the reinforced soil samples. (Figs. 10-12) show these curves for all samples.

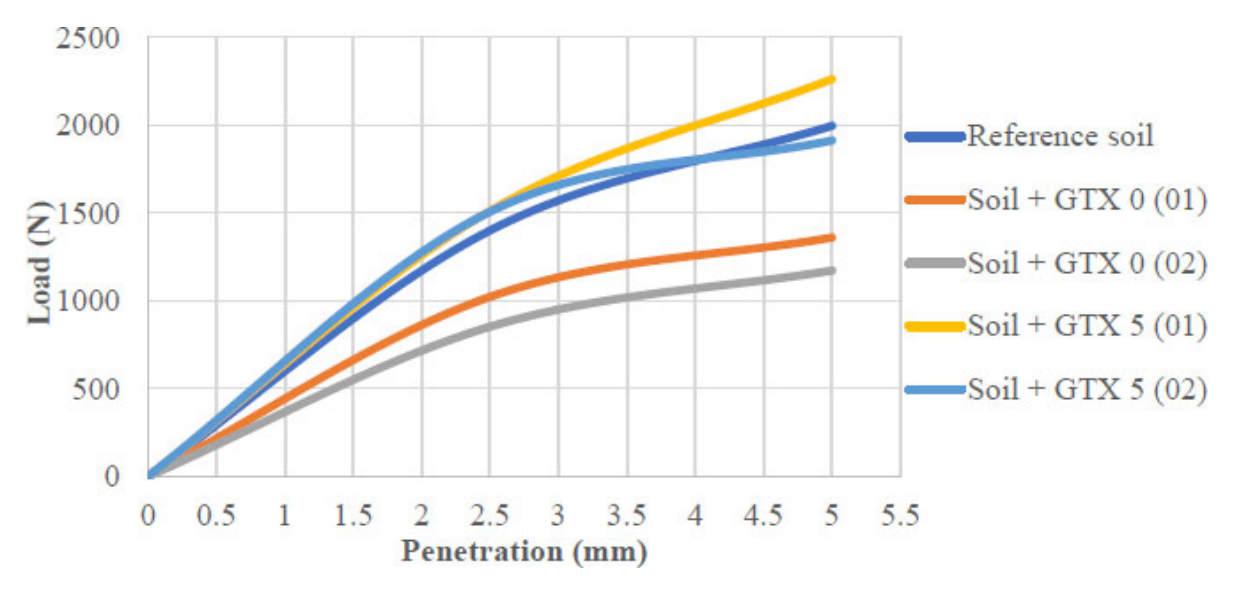


Fig. (10). Load-Penetration curves for samples compacted at 56 blows (98% of OPM).

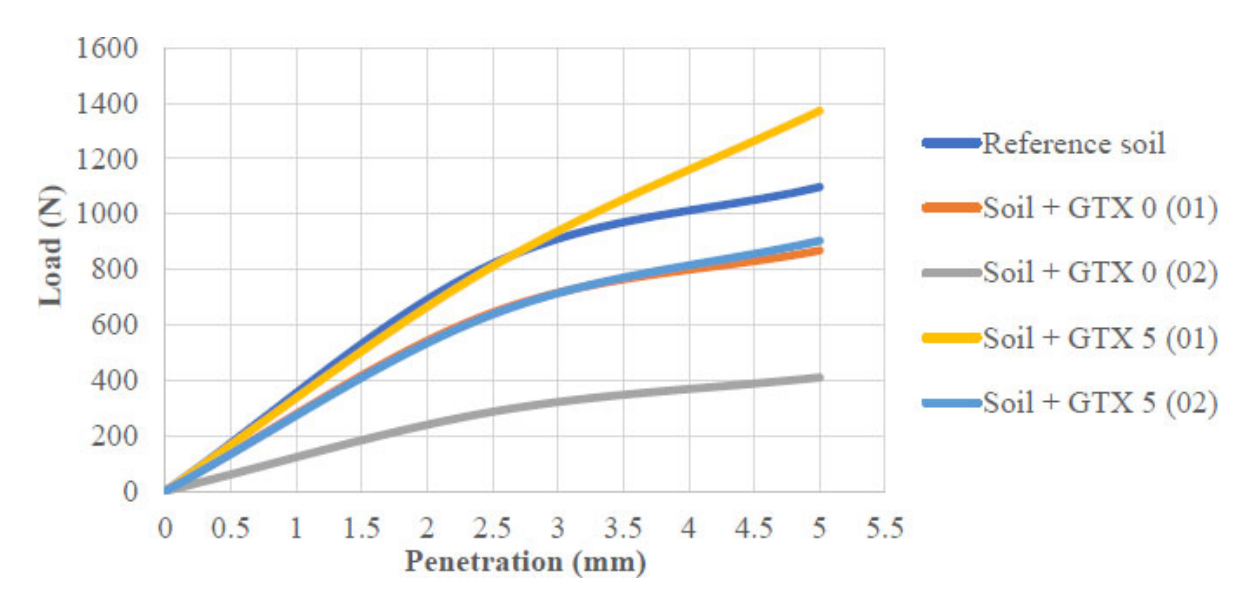


Fig. (11). Load-Penetration curves for samples compacted at 25 blows (95% of OPM).

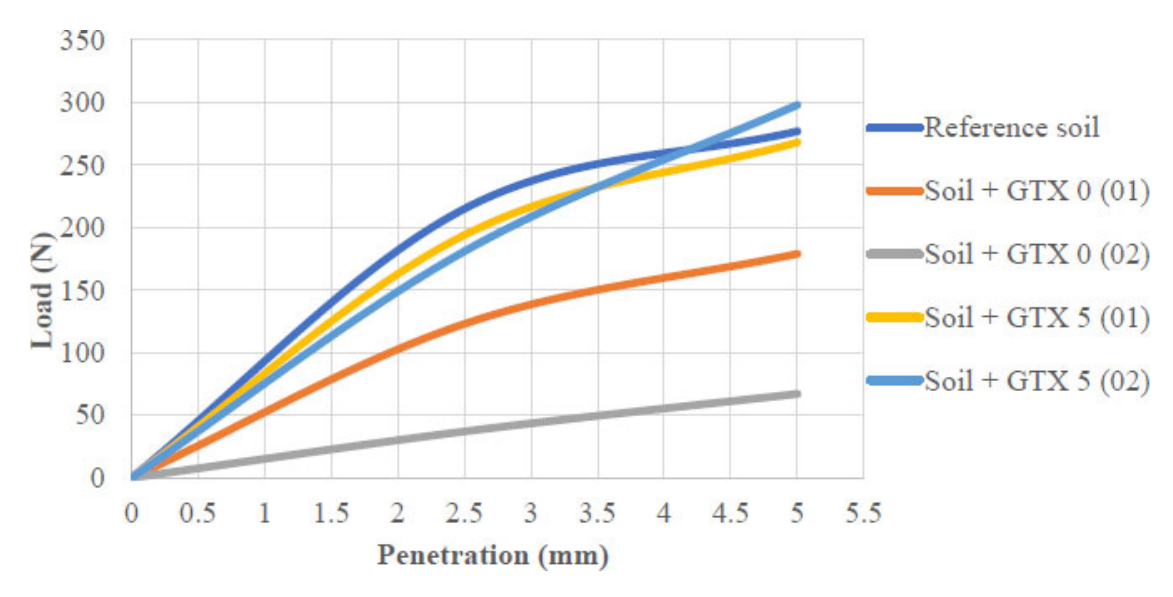


Fig. (12). Load-Penetration curves for samples compacted at 10 blows (90% of OPM).

Table 6. Synthesis of bearing capacity values.

	Bearing capacity				
Designations					
	56 blows (98% of OPM)	25 blows (95% of OPM)	10 blows (90% of OPM)		
Reference soil	90	62	14		
Soil + GTX 0 (01)	64	48	08		
Soil + GTX 0 (02)	43	22	03		
Soil + GTX 5 (01)	98	69	16		
Soil + GTX 5 (02)	88	48	13		

The graph in Fig. (10) presents the load-penetration curves for four soil samples reinforced with geotextile layers compacted at 56 blows (98% of the optimum Proctor moisture, OPM), along with a reference sample without geotextile reinforcement. The curve for the Soil + GTX 5 (01) sample exceeds that of the reference soil, indicating improved performance, with a maximum stress of 113 kPa compared with 104 kPa for the reference. The Soil + GTX 5 (02) sample initially shows a higher curve but quickly reaches its peak before declining and intersecting the curve of the unreinforced soil, although its maximum stress remains higher. In contrast, the curves for the Soil + GTX 0 (01) and Soil + GTX 0 (02) samples lie well below that of the reference soil, demonstrating no improvement when using a geotextile with a mesh opening of 0 mm.

The graph in Fig. (11) shows all the load-penetration curves for all samples compacted at 25 blows (95% of OPM). Analysis of these curves reveals that only the curve for the Soil + GTX 5 (01) sample is above that of the reference soil, indicating that at 25 blows, only this configuration resulted in an improvement in bearing capacity.

The graph in Fig. (12) presents the load-penetration curves for the different samples compacted at 10 blows

(90% of the optimum Proctor moisture, OPM), showing no significant overall improvement. However, when comparing the curves for the Soil + GTX 5 (02) sample and the reference soil, it can be observed that the Soil + GTX 5 (02) curve slightly exceeds that of the reference soil at a penetration of 4.5 mm. Similarly, the curve for Soil + GTX 5 (01) intersects that of the reference soil at a penetration of 5 mm, suggesting that these samples may exhibit better performance beyond this limit. Overall, Soil + GTX 5 (01) enhances the soil's bearing capacity, while Soil + GTX 5 (02) provides a more moderate level of reinforcement. These results are consistent with the findings of Vittalaiah et al. [2], who emphasized the influence of geotextile layer positioning within the soil.

Table 6 summarizes the bearing capacity values obtained from projections on the synthesis curves. The corresponding synthesis curves are presented in the Appendix (Annex 1-5).

In general, an increase in bearing capacity is observed for the Soil + GTX 5 (01) sample, as shown in Table 6. Adding geotextile reinforcement to soil improves its CBR index and overall strength, as shown in studies by Rudramurthy and Vikram [35]. This improvement is likely due to the openness of the geotextile mesh, which promotes better interaction between the lower layer, on

which it rests, and the upper layer. The position of the geotextile also plays a key role in this performance. Although the same type of geotextile was used for the Soil + GTX 5 (02) sample, no significant improvement was observed, which can be explained by the difference in compaction energies applied during the installation of the sheets. Conversely, a decrease in bearing capacity is observed for the other samples, in particular Soil + GTX 0 (01) and Soil + GTX 0 (02). We attribute the observed decrease in CBR strength for closed-structure geotextiles to their high compressibility and significant thickness. Under vertical loading, the internal cavities compress, resulting in material settlement and a corresponding reduction in bearing capacity. Unlike open-structure geotextiles, these geotextiles exhibit a nonlinear response, characterized by decreasing stiffness with increasing penetration.

4. DISCUSSION ON THE DURABILITY OF KENAF FIBERS

Kenaf fibers, although they exhibit attractive mechanical properties, such as good tensile strength and low density, are limited over time due to their biodegradable nature and sensitivity to environmental factors, including humidity, microorganisms, and UV radiation. This fragility reduces their durability and restricts their use in long-term applications unless they are treated or combined with other materials [12].

Indeed, the natural biodegradability of kenaf fibers, while an environmental advantage, compromises their durability when used as reinforcing materials. Over time, these fibers are subject to biological degradation processes such as rotting, fungal growth, and microbial activity, which progressively reduce their mechanical properties and, consequently, their effectiveness in structural applications. This limitation means that, without appropriate treatment, kenaf fibers are generally suitable only for short-term or temporary uses. To overcome these limitations, several treatment methods have been explored in the literature and could be adapted, including asphaltbased coating. alkaline treatment, and polymer impregnation. These different strategies aim to extend the lifespan of kenaf fibers and make their use viable in longterm contexts. However, it remains essential to preserve their ecological character, which is a fundamental criterion in the promotion of bio-sourced materials. Therefore, the real challenge lies in achieving a balance between mechanical performance and durability on the one hand, and environmental sustainability on the other [12-37].

CONCLUSION

This study investigated the feasibility of manufacturing geotextiles from kenaf fibers, a locally available raw material in Burkina Faso, for road pavement applications.

The measured physical characteristics (thickness and surface mass) show that geotextiles made from kenaf fibers could be considered for foundation layer reinforcement applications. According to SERE (1995),

geotextiles with a surface mass greater than 300 g/m^2 and 200 g/m^2 , respectively, are considered suitable for reinforcement work. In this study, the lowest surface mass value obtained was 313 g/m^2 .

Tensile and puncture tests also revealed superior performance compared to many polypropylene geotextiles intended for reinforcement. Specifically, the geotextile with a 0 mm mesh size exhibited a static puncture resistance of 1170 N and a tensile strength of up to 17.19 kN/m in the transverse direction, which is significantly higher than that of many synthetic equivalents, such as Texel SX-60T (890–1402 N/m).

Furthermore, hydraulic evaluation indicates that these geotextiles do not impede water flow, which is a crucial criterion for their reinforcement function. In terms of permeability, the geotextile with 0 mm mesh size has a surface flow rate of 2200.6 L/min/m², which is three times higher than the performance of some commercial filtration geotextiles, thereby demonstrating its capacity to maintain water flow and prevent pore clogging.

From a geotechnical perspective, the reinforcement function is well fulfilled with a geotextile layer with 5 mm openings placed at mid-height of a lateritic soil sample. The bearing capacity improves from 90 kPa (reference soil value) to 98 kPa at 98% of OPM, and from 62 to 69 kPa at 95% of OPM. This increase also highlights the important role of the geotextile mesh geometry and the role of the position of the geotextile in the reinforcement function of geotextiles.

However, the question of their durability in the soil remains a challenge. The lifespan of plant-based geotextiles typically ranges from 2 to 6 years, which limits their suitability for long-term applications. In view of this constraint, a study on treatments to enhance the durability of kenaf geotextiles could be considered to adapt them for long-term use. In order to overcome this limitation, various treatment strategies have been proposed in the literature, including asphalt-based coating, alkaline treatment, and polymer impregnation [12, 36]. These approaches are intended to enhance the durability of kenaf fibers and ensure their suitability for long-term applications. Nevertheless, it is crucial to maintain their ecological attributes, which constitute a key criterion in the advancement of bio-based construction materials. Consequently, as previously noted, the key challenge is to achieve an optimal balance between mechanical performance, long-term durability, and environmental sustainability.

AUTHORS' CONTRIBUTIONS

The authors confirm their contributions to the paper as follows: D.Y.K.T.: Study conception and design; M.F.Y. and E.W.N.: Data collection; H.F.Y. and S.M.K.: Analysis and interpretation of results; D.T.: Draft manuscript; All authors reviewed the results and approved the final version of the manuscript.

LIST OF ABBREVIATIONS

AFNOR = French Standardization Organization

CBR = California Bearing Ratio CV = Coefficient of Variation

D = Flow rate in planeDs = Specific flow rateEN = Europäische Norm

GTX = Geotextile

GTX 0 = 0 mm mesh opening geotextile

 $GTX \ 0 \ (01) = 0 \ mm \ geotextile layer$

 $GTX \ 0 \ (02) = Two \ 0 \ mm \ geotextile layers$

GTX 5 = 5 mm mesh opening geotextile

GTX 5 (01) = 5 mm geotextile layer

GTX 5 (02) = Two 5 mm geotextile layers

ISO = International Organization for

Standardization

NF = French Norm

Q = Volume of water (m³) poured into the

funnel

R = Tensile strength RN4 = National Road N°4

S = Geotextile sample surface area

s = Surface area of the lower end of the funnel

t = Time

 ε = Deformation

 γ_{dmax} = Maximum dry unit weight

 ω_{opt} = Optimum water content

 Δ l = Elongation

CONSENT FOR PUBLICATION

Not applicable.

AVAILABILITY OF DATA AND MATERIALS

All data generated or analyzed during this study are included in this published article.

FUNDING

This study was funded by the National Fund for Research and Innovation for Development (FONRID).

CONFLICT OF INTEREST

The authors confirm that this article's content has no conflict of interest.

ACKNOWLEDGEMENTS

The authors express their gratitude to the National Fund for Research and Innovation for Development (FONRID) for the financial support provided to the "Geosynthetics project".

APPENDIX

Annex 1: Synthesis curve of the reference soil - reference soil

Annex 2: Synthesis curve of soil sample + GTX (01)

Annex 3: Synthesis curve of soil sample+ GTX 0 (02)

Annex 4: Synthesis curve of soil sample + GTX 5 (01)

Annex 5: Synthesis curve of soil sample + GTX 5 (02)

REFERENCES

[1] V.K. Thakur, M.K. Thakur, and R.K. Gupta, "Review: Raw natural fiber-based polymer composites", *IJPAC Int. J. Polym. Anal. Charact.*, vol. 19, no. 3, pp. 256-271, 2014. [http://dx.doi.org/10.1080/1023666X.2014.880016]

[2] A. Vittalaiah, A. Prakash, and R. Ravinder, "Effect of geotextile on CBR strength of unpaved road with soft subgrade", 6th National conference NCWES-2019, 2019

[3] A. Huckert, "Experimental and numerical approaches to the design of geosynthetic reinforcements on cavities and rigid inclusions", PhD thesis, University of Grenoble, 2014.

[4] C. La Borderie, and D. Breysse, "Study of differential settlement on heterogeneous soils", European J. Civil. Eng., vol. 11, pp. 453-462, 2007.

[http://dx.doi.org/10.1080/17747120.2007.9692939]

[5] J.C. Quezada, "Mechanisms of ballast settlement and its variability", PhD thesis, University of Montpellier 2, 2014.

[6] M.T.M. Mbengue, "Geo-mechanical characterization of raw and treated soils for better use in road construction: The case of the Saaba and Kamboinsé borrow pits in Burkina Faso", Doctoral dissertation. University of Le Havre Normandy, 2023.

[7] B. Simon, L. Briançon, and L. Thorel, "Soil improvement by rigid inclusions: the role of geosynthetics in the load transfer platform", French J. Geotech., vol. 162, pp. 1-27, 2020.

[http://dx.doi.org/10.1051/geotech/2020003]

[8] N. Touze, "The contribution of geosynthetics to sustainable development", French J. Geotechnics, vol. 160, pp. 1-19, 2019. [http://dx.doi.org/10.1051/geotech/2019018]

[9] D. Jin, D. Ge, X. Zhou, and Z. You, "Asphalt mixture with scrap tire rubber and nylon fiber from waste tires: laboratory performance and preliminary M-E design analysis", *Build.*, vol. 12, no. 2, p. 160, 2022.

[http://dx.doi.org/10.3390/buildings12020160]

[10] E. Bocci, and E. Prosperi, "Recycling of reclaimed fibers from endof-life tires in hot mix asphalt", *J. Traffic Transp. Eng.*, vol. 7, no. 5, pp. 678-687, 2020. [English Edition]. [http://dx.doi.org/10.1016/j.jtte.2019.09.006]

[11] D. Ge, Z. You, S. Chen, C. Liu, J. Gao, and S. Lv, "Laboratory performance and field case study of asphalt mixture with sasobit treated aramid fiber as modifier", *Transp. Res. Rec.*, vol. 2675, no. 12, pp. 637-649, 2021.

[http://dx.doi.org/10.1177/03611981211047833]

[12] J. Wang, Y. Xiong, Q. Li, D. Jin, Y. Hu, and T. Che, "Experimental investigation on the preparation and surface treatment of biomass fibers for stone mastic asphalt mixtures modification", *Constr. Build. Mater.*, vol. 408, p. 133667, 2023. [http://dx.doi.org/10.1016/j.conbuildmat.2023.133667]

[13] M. Bessaim, A. Bessaim, H. Missoum, and K. Bendani, "Soil reinforcement with geosynthetics", MATEC Web. Conf., vol. 149, no. 02096, pp. 1-3, 2018.

[14] H.M. Akil, M.F. Omar, A.A.M. Mazuki, S. Safiee, Z.A.M. Ishak, and A. Abu Bakar, "Kenaf fiber reinforced composites: A review", *Mater. Des.*, vol. 32, no. 8-9, pp. 4107-4121, 2011. [http://dx.doi.org/10.1016/j.matdes.2011.04.008]

[15] S. Gwon, S.H. Han, T.D. Vu, C. Kim, and M. Shin, "Rheological and mechanical properties of kenaf and jute fiber-reinforced

- cement composites", *Int. J. Concr. Struct. Mater.*, vol. 17, no. 1, p. 5, 2023.
- [http://dx.doi.org/10.1186/s40069-022-00565-1]
- [16] N.M. Nurazzi, M.R.M. Asyraf, S. Fatimah Athiyah, S.S. Shazleen, S.A. Rafiqah, M.M. Harussani, S.H. Kamarudin, M.R. Razman, M. Rahmah, E.S. Zainudin, R.A. Ilyas, H.A. Aisyah, M.N.F. Norrrahim, N. Abdullah, S.M. Sapuan, and A. Khalina, "A review on mechanical performance of hybrid natural fiber polymer composites for structural applications", *Polymers*, vol. 13, no. 13, p. 2170, 2021. [http://dx.doi.org/10.3390/polym13132170] [PMID: 34209030]
- [17] Y. Millogo, J.E. Aubert, E. Hamard, and J.C. Morel, "How properties of kenaf fibers from Burkina Faso contribute to the reinforcement of earth blocks. Univers", *Materials*, vol. 8, no. 5, pp. 2332-2345, 2015. [http://dx.doi.org/10.3390/ma8052332]
- [18] S.S. Muthu, "Roadmap to sustainable textiles and clothing: Ecofriendly raw materials, technologies, and processing methods", In: *Textile Science and Clothing Technology.*, Springer Singapore, 2014. [http://dx.doi.org/10.1007/978-981-287-065-0]
- [19] A. Séré, "Structures reinforced with geotextiles loaded at the top: Behavior and design", PhD thesis, National School of Bridges and Roads. 1995.
- [20] I. Madani, and S. Khetout, "Study and design of spinning and weaving devices", Master thesis, Mohamed Boudiah University of M'Sila 2023
- [21] R. Shivashankar, and J. Jayaraj, "Behaviour of prestressed geosynthetic reinforced granular beds overlying weak soil", *Indian Geotechn. J.*, vol. 44, no. 1, pp. 26-38, 2014. [http://dx.doi.org/10.1007/s40098-013-0070-6]
- [22] M. Kapor, A. Skejić, S. Medić, and A. Balić, "Experimental evaluation of relative soil-geotextile displacements induced by strip footing pressure on a reinforced foundation bed over soft subgrade", Int. J. Geosynthet. Ground Eng., vol. 9, no. 6, p. 82, 2023.
- [23] M.A. Adajar, "The use of woven geotextile for settlement reduction of spread footing on granular soil", Int. J. GEOMATE, vol. 16, no. 58, pp. 211-217, 2019.

[http://dx.doi.org/10.21660/2019.58.8122]

[http://dx.doi.org/10.1007/s40891-023-00503-5]

- [24] P. Kumar, K. Gaur, and A. Trivedi, "Strength analysis of geotextile-reinforced subgrade", In: Advances in Geotechnical Engineering, Springer: Singapore, 2024, pp. 475-489. [http://dx.doi.org/10.1007/978-981-99-8505-0_25]
- [25] T. Shil, and S. K. Pal, "Influence of millet-based diet on glycemic control and antioxidant status: a nutraceutical perspective", *Mater Today Proc*, vol. 92, pp. 3114-3119, 2023.

- [http://dx.doi.org/10.1016/j.matpr.2023.11.042]
- [26] A. Shrivastava, and A. Sachan, "Application of bioinformatics in understanding metabolic pathways of probiotics", In: Probiotics and Prebiotics in Human Nutrition and Health, Springer: Singapore, 2022, pp. 229-242. [http://dx.doi.org/10.1007/978-981-33-6466-0 13]
- [27] "Technical data sheet Texel SX Reinforcement 1 and SX filtration", Available from: https://texel.ca/fileadmin/medias/documents/en/geosynthetics/spe cifications-sheets/geotextiles/FICHE_TECHNIQUE_-_SX-Reinforcement_1_SX-Filtration_-_ENG_20240415.pdf
- [28] N.M. Kibwela, and D.Y. Mande, "Comparative study of mechanical properties of a polymer matrix composite material reinforced with bamboo and date palm vegetable fibers", Master thesis, University of Lubumbash, 2023.
- [29] M. Ouedraogo, K. Dao, Y. Millogo, M. Seynou, J.-E. Aubert, and M. Gomina, "Influence kenaf fibers (Hibiscus altissima) on the physical and mechanical properties of adobes", J. the West African Chem. Societ, pp. 48-63, 2017.
- [30] S. Lambert, "Geotextiles: Functions, characteristics and sizing", Water. Territorial Sci., vol. 22, p. 17, 2010.
- [31] A.K. Ashmawy, and P.L. Bourdeau, "Response of a woven and a nonwoven geotextile to monotonic and cyclic simple tension", *Geosynth. Int.*, vol. 3, no. 4, pp. 493-515, 1996. [http://dx.doi.org/10.1680/gein.3.0072]
- [32] "Geotextile catalog: Nonwoven geotextile specifications",
 Available from:
 https://www.walcoom.com/pdf/geotextile-catalog.pdf
- [33] "800g non-woven geotextile filter fabric for erosion protection", Available from: https://www.geotextile-fabric.com/quality-6945217-800g-non-woven-geotextile-filter-fabric-erosion-protection-environmental
- [34] "Sikaplan®-800 product datasheet", Available from: https://can.sika.com/en/construction/shotcrete-tunnelingmining/w aterproofing-products/sikaplan-system/geotextiles-anddrainage/sikaplan-800-geotextile.html
- [35] M. Rudramurthy, and M.B. Vikram, "Effect of geotextiles on CBR values", Int. J. Emerg. Trend. Eng. Develop., vol. 1, no. 6, pp. 118-126, 2018.
- [36] L. Xie, H. Zhang, and J. Li, "Investigation of surface modification of bagasse fibers for improved performance in asphalt mixtures", *Buildings*, vol. 14, no. 5, p. 1352, 2024. [http://dx.doi.org/10.3390/buildings14051352]
- [37] Z. Liao, Y. Hu, Y. Shen, K. Chen, C. Qiu, J. Yang, and L. Yang, "Investigation into the reinforcement modification of natural plant fibers and the sustainable development of thermoplastic natural plant fiber composites", *Polymers*, vol. 16, no. 24, p. 3568, 2024. [http://dx.doi.org/10.3390/polym16243568] [PMID: 39771421]

DISCLAIMER: The above article has been published, as is, ahead-of-print, to provide early visibility but is not the final version. Major publication processes like copyediting, proofing, typesetting and further review are still to be done and may lead to changes in the final published version, if it is eventually published. All legal disclaimers that apply to the final published article also apply to this ahead-of-print version.